Structure of the cold-shock domain protein from *Neisseria meningitidis* reveals a strand-exchanged dimer

**Jingshan Ren,[a,b] Joanne E.
Nettleship,[a] Sarah Sainsbury,[a]
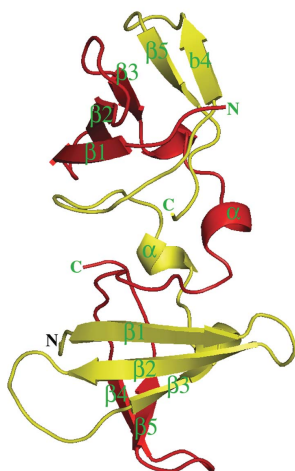Nigel J. Saunders[c] and
Raymond J. Owens[a]***

[a]The Oxford Protein Production Facility, Henry
Wellcome Building for Genomic Medicine,
University of Oxford, Roosevelt Drive,
Oxford OX3 7BN, England, [b]Division of
Structural Biology, Henry Wellcome Building for
Genomic Medicine, University of Oxford,
Roosevelt Drive, Oxford OX3 7BN, England,
and [c]Bacterial Pathogenesis and Functional
Genomics Group, Sir William Dunn School of
Pathology, University of Oxford, South Parks
Road, Oxford OX1 3RE, England

Correspondence e-mail: ray@strubi.ox.ac.uk

The structure of the cold-shock domain protein from *Neisseria meningitidis* has been solved to 2.6 Å resolution and shown to comprise a dimer formed by the exchange of two β-strands between protein monomers. The overall fold of the monomer closely resembles those of other bacterial cold-shock proteins. The neisserial protein behaved as a monomer in solution and was shown to bind to a hexathymidine oligonucleotide with a stoichiometry of 1:1 and a K_d of 1.25 μM.

1. Introduction

The human pathogen *Neisseria meningitidis* is a Gram-negative bacterium that is responsible for bacterial meningitis and septicaemia. Sequencing and annotation of the *N. meningitidis* serotype B genome (strain MC58) revealed a putative cold-shock gene (NMB0838) predicted to encode a 7.2 kDa acidic protein with high sequence similarity to other bacterial cold-shock proteins (Csps; Tettelin *et al.*, 2000). Expression of Csps in bacteria is induced under a range of growth conditions, most notably in response to cold stress; they are essential for growth at low temperatures (Thieringer *et al.*, 1998). Amongst the most well studied Csps is the major cold-induced protein in *Escherichia coli*, CspA, which functions as an RNA chaperone binding nonspecifically to RNA and ssDNA (Jiang *et al.*, 1997). At low temperature, RNA forms stable secondary structures and it has been proposed that CspA (and other Csps) enhances translation by eliminating stabilized RNA secondary structures (Jiang *et al.*, 1997). Csps also appear to function as transcription antiterminators, providing a mechanism for controlling the expression of other cold-shock-induced genes (Bae *et al.*, 2000).

The structures of a number of Csps have been determined by either X-ray crystallography or NMR, namely *E. coli* CspA (*Ec*-CspA; Schindelin *et al.*, 1994; Newkirk *et al.*, 1994), *Bacillus subtilis* CspB (*Bs*-CspB; Schnuchel *et al.*, 1993), *B. caldolyticus* Csp (*Bc*-Csp; Mueller *et al.*, 2000) and *Thermotoga maritima* Csp (Kremer *et al.*, 2001). All show an OB (oligonucleotide/oligosaccharide-binding) fold consisting of five antiparallel β-strands forming a β-barrel structure. The oligonucleotide-binding region of Csps has been mapped to two conserved sequence motifs, RNP-1 and RNP-2, located on adjacent β-strands (Schroder *et al.*, 1995). These sequences are characteristic of many RNA-binding proteins (Landsman, 1992) and comprise a high proportion of basic and aromatic residues. The structures of CspB from *Bacillus subtilis* and Csp from *B. caldolyticus* in complex with hexathymidine (dT$_6$) have been reported (Max *et al.*, 2006, 2007). Both structures show that oligonucleotide binding involves stacking interactions between phenylalanine residues and the thymidine base, together with hydrogen bonds between the side chains of polar amino acids and pyrimidine bases. The residues involved in the interaction surface of Csps from *Bacillus* are conserved within the *Neisseria* NMB0838 gene product, implying that this protein may also bind ssDNA in a similar way to CspB. In this report, we describe the production of the neisserial Csp (referred to as *Nm*-Csp), analysis of ssDNA binding and structure determination by X-ray crystallography.

2. Materials and methods

2.1. Protein production and crystallization

The NMB0838 gene was amplified by PCR using *N. meningitidis* genomic DNA (strain MC58) as a template and primers designed for ligation-independent cloning *via* In-Fusion technology (Clontech). PCR with KOD HiFi polymerase (Merck) used the forward and reverse primers 5′-AAGTTCTGTTTCAGGGCCCGATGGCAAC-CGGTATCGTAAAATGG-3′ and 5′-ATGGTCTAGAAAGCTTTA-TTAGGCCTGAATGTTGGCGG-3′, respectively. The PCR product was purified using QIAquick 96 plates (Qiagen) and inserted into the vector pOPINB using the protocol of Berrow *et al.* (2007). The expression construct contained an N-terminal His tag and a 3C protease cleavage site (bold): MGSSHHHHHHSSG**LEVLFQGP**. Recombinant clones were identified by PCR with the gene-specific forward primer and a T7 reverse primer and were verified by DNA sequencing.

Both native and selenomethionine-labelled *Nm*-Csp were produced in *E. coli* strain B834 (DE3) using the auto-induction method (Studier, 2005). Native protein was expressed in Overnight Express Instant TB media (Merck) and selenomethionine-labelled protein was produced in a glucose-free version of the SelenoMet media (Molecular Dimensions) in conjunction with Overnight Express System 1 (Merck). Cells were grown in 2 l cultures at 310 K for 4 h and the temperature was then lowered to 298 K. Following incubation for a further 20 h, the cells were harvested by centrifugation for 15 min at 6000g and lysed using a Basic Z Cell Disruptor (Constant Systems) at 207 MPa in the presence of 50 mM Tris pH 7.5, 500 mM NaCl, 0.2% Tween-20, 10 µg ml^{-1} DNAse and an EDTA-free protease inhibitor cocktail tablet (Roche). The lysate was centrifuged at 16 000g for 30 min to remove cell debris before loading the soluble fraction onto a 1 ml HisTrap FF column (GE Healthcare). The column was washed with 50 mM Tris pH 7.5, 500 mM NaCl, 20 mM imidazole before elution of the protein with 50 mM Tris pH 7.5, 500 mM NaCl, 500 mM imidazole. The protein was then injected onto a 16/60 HiLoad Superdex 75 column (GE Healthcare) and eluted with 20 mM Tris pH 7.5, 200 mM NaCl. Protein-containing fractions were analysed by SDS–PAGE (NuPage, Invitrogen). The N-terminal tag was removed by incubation overnight at 277 K with His-tagged 3C protease (prepared from a pET24a/His3C expression vector kindly donated by A. Geerlof, EMBL, Hamburg). The 3C protease and any uncleaved protein were removed by nickel-affinity chromatography and the protein was concentrated to 40 mg ml^{-1} using a 2 kDa molecular-weight cutoff Vivaspin 15R concentrator (Sartorius). The quality of the protein sample and the seleno-methionine incorporation were analysed by electrospray mass spectrometry (Geerlof *et al.*, 2006).

Native protein crystals were obtained in a 200 nl sitting-drop vapour-diffusion crystallization experiment in 0.8 M sodium dihydrogen phosphate, 1.2 M dipotassium hydrogen phosphate, 100 mM acetate pH 4.5 with a final pH of 6.7 (condition No. 35 of Emerald Wizard II Screen; Emerald Biosystems; Walter *et al.*, 2005). Seleno-methionine-labelled protein crystals were obtained by cross-seeding with native crystals using the same crystallization condition according to the protocol of Walter *et al.* (2008).

2.2. Data collection, structure determination and refinement

Multiple-wavelength anomalous dispersion data were collected to 2.6 Å resolution from a selenomethionine-labelled *Nm*-Csp crystal on beamline BM14 at the ESRF (Grenoble, France). Following a fluorescence scan, 360° of X-ray data at the peak wavelength (0.979 Å)

Table 1
X-ray data-collection and refinement statistics.

(*a*) Data-collection details. Values in parentheses are for the highest resolution shell.

Data set	Peak	Remote
X-ray source	ESRF BM14	
Wavelength (Å)	0.979	0.907
Space group	$P4_12_12$	
Unit-cell parameters (Å)	$a = b = 59.37$, $c = 89.42$	
Resolution range (Å)	30.0–2.60 (2.69–2.60)	30.0–2.80 (2.90–2.80)
Unique reflections	5271 (459)	4299 (412)
Completeness (%)	98.5 (88.8)	99.7 (98.8)
Redundancy	23.9 (13.1)	12.7 (10.0)
Average $I/\sigma(I)$	29.2 (1.7)	17.9 (1.3)
R_{merge}	0.127 (0.834)	0.137 (0.957)

(*b*) Refinement statistics.

Resolution range (Å)	30.0–2.60
No. of reflections (working/test)	4951/270
R factor (R_{work}/R_{free})	0.233/0.296
No. of atoms (protein/water)	1014/16
R.m.s. bond-length deviation (Å)	0.008
R.m.s. bond-angle deviation (°)	1.0
Mean B factor (protein/water) (Å^2)	72/63

and 180° at a remote wavelength (0.907 Å) were collected with an oscillation of 1.0° per frame. Crystals taken directly from the crystallization drop without the addition of a cryoprotectant were flash-frozen and maintained at 100 K under a stream of nitrogen gas during data collection. Indexing and integration of data images were carried out using *HKL*-2000. The statistics of the X-ray data are given in Table 1.

The *Nm*-Csp crystal belongs to space group $P4_12_12$, with unit-cell parameters $a = b = 59.37$, $c = 89.42$ Å. There are two monomers in the crystal asymmetric unit, with a solvent content of 53%. The *SHELX* program suite was used to evaluate the anomalous signal during the course of the MAD data collection and to solve the positions of the selenium sites. *SOLVE*/*RESOLVE* (Terwilliger, 2000; Terwilliger & Berendzen, 1999) were then used for refinement of the selenium positions and phase improvement combined with automated model building. The model partially built by *RESOLVE* was rebuilt manually using the program *O* (Jones *et al.*, 1991) and then refined with *CNS* (Brünger *et al.*, 1998) using simulated annealing and positional refinement with main-chain NCS restraints followed by individual isotropic *B*-factor refinement. There are apparent structural differences in the N-terminal part (residues 1–27) between the two monomers which were not included in the NCS restraints. The structure was finally refined with *REFMAC* and the statistics for the structure are given in Table 1.

2.3. Analytical size-exclusion chromatography

200 µl of 1 mg ml^{-1} selenomethionine-labelled protein was loaded onto a Superdex 75 10/300 GL column (GE Healthcare) equilibrated in 20 mM Tris pH 7.5, 200 mM NaCl. Elution of the protein in 20 mM Tris pH 7.5, 200 mM NaCl was detected by UV absorbance (A_{280} and A_{254}). A further sample of protein was incubated with the single-stranded DNA fragment dT$_6$ in a 1:1 molar ratio at room temperature for 30 min before analysis by analytical size-exclusion chromatography as described above. The column was calibrated using a Gel Filtration LMW Calibration Kit (GE Healthcare).

2.4. Fluorescence titration DNA-binding assay

The fluorescence of Trp8 in *Nm*-Csp was measured using a Shimadzu RF-1501 spectrofluorophotometer. Experiments were

carried out at room temperature in 20 m*M* Tris pH 7.5, 200 m*M* NaCl. 0.25 µ*M* protein solution was titrated with increasing amounts of dT$_6$ from 0 to 20 µ*M*. The samples were gently stirred and after 2 min incubation the fluorescence of Trp8 was excited at 280 nm and measured at 343 nm. The initial volume was 600 µl and the increase in volume after the addition of concentrated DNA solution was 2% or less. The fluorescence was corrected for buffer fluorescence, filter effects and DNA autofluorescence. The effect of random collisions to the fluorescence reading was eliminated by repeating the titration with 40 µ*M* *N*-acetyltryptophanamide (data not shown). The fluorescence-quenching data revealed a binding isotherm from which K_d, the dissociation constant of the complex, and *n*, the stoichiometry of the protein–DNA complex (the number of protein molecules bound to one ssDNA molecule), were calculated using the nonlinear regression software package *Prism* 5 (GraphPad Software Inc.).

3. Results and discussion

3.1. Overall structure

The X-ray crystal structure of the cold-shock domain protein from *N. meningitidis* (*Nm*-Csp) was determined by multiple-wavelength anomalous dispersion using selenomethionine-substituted protein. Despite high sequence homology to *Ec*-CspA and *Bs*-CspB, solution by molecular replacement did not prove to be possible owing to the novel arrangement of the protein described below. The structure reveals that two polypeptide chains from *Nm*-Csp form a dimer in the crystallographic asymmetric unit consisting of two five-stranded β-barrels (Fig. 1*a*). Superimpositions of the monomers of *Nm*-Csp with those of *Ec*-CspA (PDB code 1mjc) and *Bs*-CspB (PDB code 2es2) gave r.m.s.d.s of 1.1 and 1.2 Å for 66 and 63 equivalent C$^\alpha$ atoms out of 67, respectively, confirming the high degree of structural conservation of the Csp fold. However, in both *Ec*-CspA and *Bs*-CspB each chain is folded into an independent three-dimensional

biological unit, whereas in *Nm*-Csp each monomer is composed of residues from two chains: the N-terminal residues 1–36 are from one chain and the C-terminal residues 37–67 are from the other (Figs. 1*a* and 1*b*). At the point of transition, residues Met36, Glu37 and Gly38 of each subunit form a single α-helical turn. This results in the two phenylalanine residues at position 39 of the subunits being buried in the core of the dimer, forming a potential ring-stacking interaction (Fig. 1*b*). This contrasts with the monomeric structures of *Ec*-CspA and *Bs*-CspB, in which the side chains of the equivalent residues are exposed at the surface of the proteins. Domain swapping has recently been observed in the structure of Csp from *B. caldolyticus* (*Bc*-Csp) in complex with a hexathymidine ligand (Max *et al.*, 2007). The point of exchange was the same as in *Nm*-Csp, but the relative orientation and separation of the two monomers in the *Bc*-Csp structure is very different. As shown in Fig. 1(*c*), only one of the two domain-swapped monomers can be overlaid. This appears to be entirely a consequence of the methionine at position 36 in *Nm*-Csp, which favours the formation of the short helical turn. In contrast, the glycine at this position in *Bc*-Csp results in a more extended hinge-loop region between the monomers and the exposure of the equivalent of Phe39 at the surface of the protein as observed in *Ec*-CspA and *Bs*-CspB. Interestingly, as in the *Bs*-CspB–ssDNA complex structure, this phenylalanine residue is involved in the interaction between the protein and the oligonucleotide ligand d(T)$_6$ (Max *et al.*, 2007, 2006). The residues that are involved in the binding of oligonucleotides in *Bs*-CspB and *Bc*-Csp (Max *et al.*, 2006, 2007) are highly conserved in *Nm*-Csp (Fig. 2), implying that the protein would bind to ssDNA oligonucleotides in the same way as the *Bacillus* Csps. However, the fact that one of the hydrophobic residues (Phe39) that form the binding surface is buried in the *Nm*-Csp structure suggests that binding to the domain-swapped dimer may be compromised. Domain swapping has been noted in a variety of different proteins, with the swapped domains showing diverse secondary structures (Liu & Eisenberg, 2002; Bennett *et al.*, 1995). The functional significance of
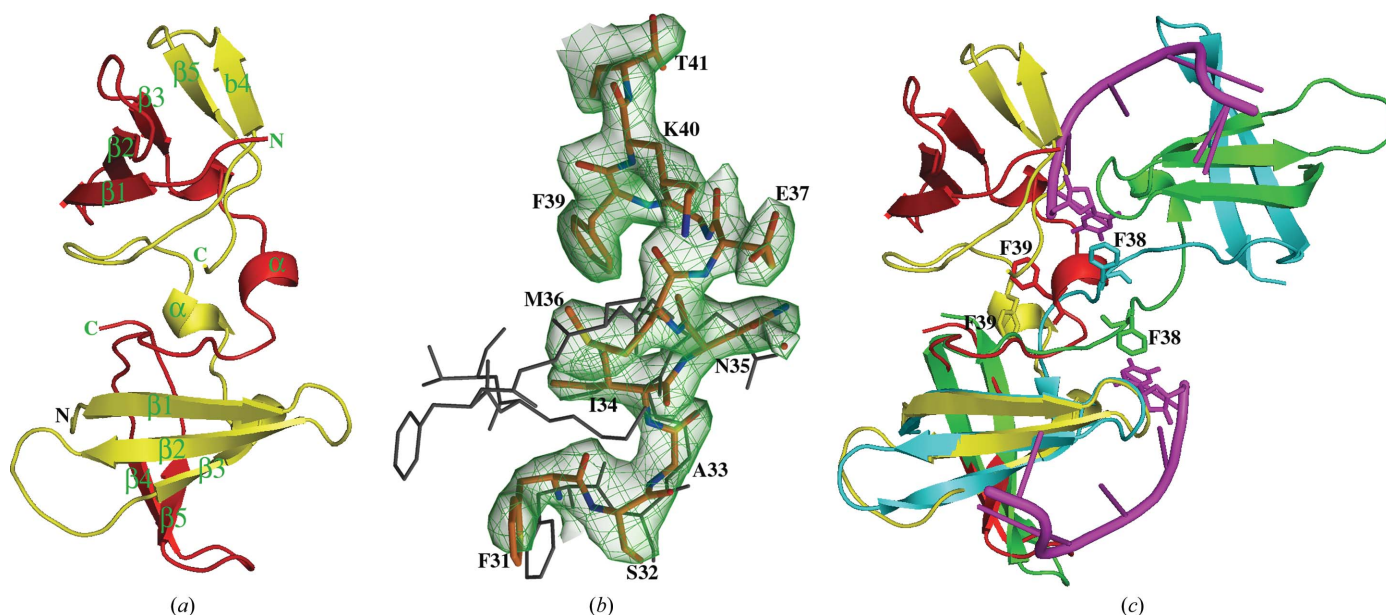

Figure 1
The structure of *Nm*-Csp and comparison with *Bc*-Csp. (*a*) Ribbon diagram showing the *Nm*-Csp dimer in the crystallographic asymmetric unit; the two polypeptide chains are coloured yellow and red and secondary-structure features are numbered. (*b*) |2*F*$_o$| − |*F*$_c$| map contoured at 1.2σ showing electron density for residues 31–41 where chain switching occurs between monomers of *Nm*-Csp. The *Nm*-Csp residues, which are labelled and shown in stick format, are superimposed onto the equivalent region of *Bs*-CspB (PDB code 2es2) shown as black lines. (*c*) Overlay of the *Nm*-Csp dimer, coloured red and yellow, with that of *Bc*-Csp (PDB code 2hax), coloured green and turquoise, bound to oligo-dT (coloured purple). The positions of the Phe38 residues involved in nucleotide base stacking in *Bc*-Csp and the corresponding Phe39 residues in *Nm*-Csp are shown.
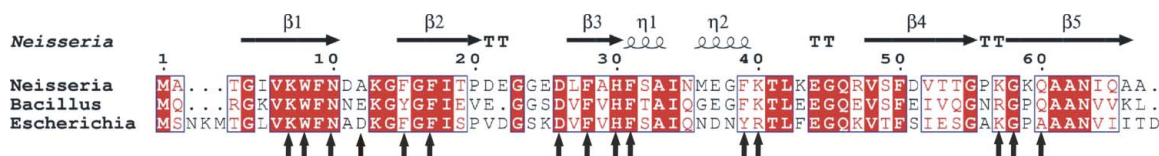
Figure 2
Structure-based alignment of cold-shock proteins (Csps). The sequences of *N. meningitis* Csp (*Nm*-Csp), *E. coli* CspA (*Ec*-CspA) and *B. caldolyticus* Csp (*Bc*-Csp) were aligned using *ClustalW* and displayed with secondary structures using *ESPript*2.2. The key residues involved in the DNA binding of *Bacillus* Csps are indicated by arrows.

these phenomena depends upon the protein and in some cases arises as an artifact *in vitro*. However, it has been noted that the formation of secondary structure in the hinge region involved in domain exchange indicates that the dimer is relatively more stable than the monomeric form of the protein (Liu & Eisenberg, 2002).

3.2. DNA binding

Analytical size-exclusion chromatography (SEC) and fluorescence titration experiments were used to investigate the DNA-binding properties of *Nm*-Csp. The oligonucleotide dT_6 was chosen as Max and coworkers have reported the structures of *Bs*-CspB and *Bc*-Csp with this single-stranded DNA incorporated into the DNA-binding site (Max *et al.*, 2006, 2007). During analytical size-exclusion chromatography, purified *Nm*-Csp eluted as an 8 kDa monomeric protein (Fig. 3), in contrast to the crystallized protein, which is dimeric. Following incubation of the protein with hexathymidine (dT_6) in a 1:1 molar ratio, the elution peak shifted to around 13 kDa (Fig. 3), indicating the formation of a complex between *Nm*-Csp and the single-stranded DNA oligomer. The ratio A_{254}/A_{280} in the eluted peak increased from 2.94 to 9.91, which is consistent with the presence of DNA in the sample after complex formation. The 5 kDa shift of the elution peak is larger than would be expected for a globular complex comprising one *Nm*-Csp monomer (8 kDa) and one oligomer of dT_6 (corresponding to a molecular weight of 1.4 kDa). However, oligonucleotides behave on gel-filtration columns as though four to five times larger than globular proteins of corresponding molecular weight (Kim *et al.*, 2007). Therefore, we attribute the discrepancy in the size of the complex to the presence of the oligonucleotide and
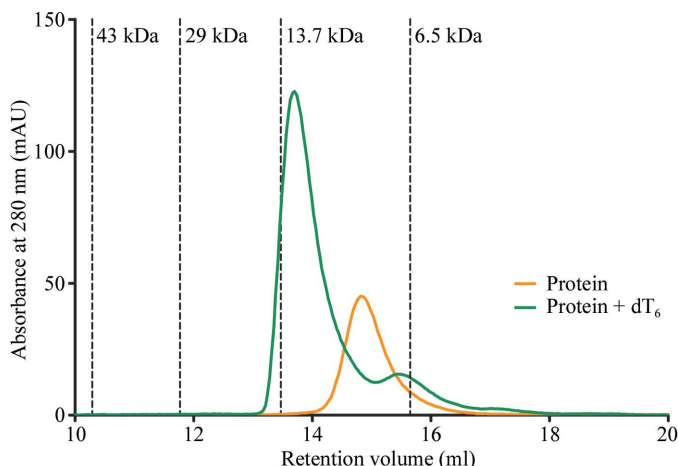
conclude that *Nm*-Csp forms a monomeric complex with ssDNA. Further experiments, for example using analytical ultracentrifugation, would be required to confirm this result.

The stoichiometry n and the dissociation constant K_d of the protein–oligonucleotide complex were obtained using a fluorescence titration experiment which measures the fluorescence quenching of Trp8 upon DNA binding (Max *et al.*, 2006; Zeeb & Balbach, 2003). Trp8 forms part of the RNP1 nucleic acid binding motif (Landsman, 1992; Schroder *et al.*, 1995). The number of protein molecules bound to each dT_6 molecule, n, was calculated to be 0.99 ± 0.01, indicating 1:1 binding of the DNA to the protein (Fig. 4). The K_d for the protein–oligonucleotide complex was calculated to be $1.25 \pm 0.04\ \mu M$ (Fig. 4). This compares with a K_d of $0.32 \pm 0.02\ \mu M$ for the wild-type *Bs*-CspB–dT_6 complex (Zeeb *et al.*, 2006), indicating that *Nm*-Csp binds dT_6 less strongly than *Bs*-CspB. All the hydrophobic residues that form the DNA-binding surface in the *Bs*-CspB complex are conserved in the *Nm*-Csp sequence; the only differences among the DNA-contact residues are alanine for glutamate at position 12 and lysine for arginine at position 56 (Fig. 2). It is not clear that these differences would account for the reduced binding.

4. Conclusions

We have described the crystallographic structure of *Nm*-Csp at 2.6 Å resolution. The structure comprises a dimer with each subunit built of residues from two separate chains; this is in contrast to the *Ec*-CspA and *Bs*-CspB structures reported previously (Schindelin *et al.*, 1994; Schnuchel *et al.*, 1993), but similar to the structure of *Bc*-Csp (Max *et al.*, 2007). This suggests that Csp proteins may have a propensity to undergo domain swapping to form metastable dimeric structures. The
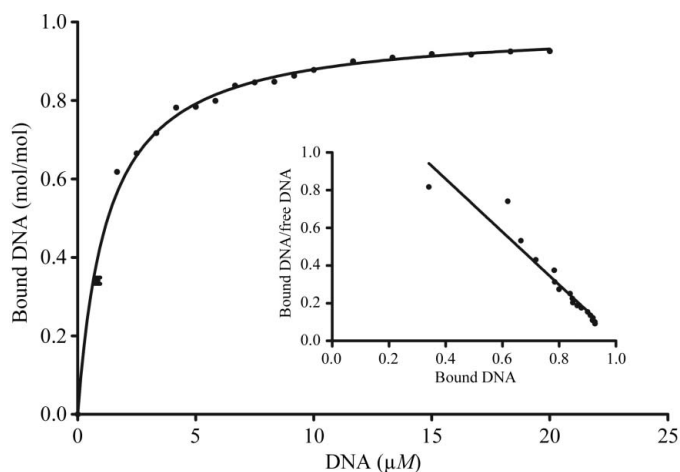

Figure 3
Analysis of *Nm*-Csp by size-exclusion chromatography with and without single-stranded DNA (107 µg). Overlaid size-exclusion chromatograms (each using 200 µg of protein) showing the monomeric *Nm*-Csp (orange trace) eluting at 14.8 ml and the *Nm*-Csp–dT_6 heterodimer eluting at 13.6 ml (green trace). The elution volumes of the calibrants along with their molecular weights are represented by vertical dotted lines. The A_{254}/A_{280} ratios for the eluted peaks were 2.94 for the protein alone and 9.91 for the protein plus oligonucleotide.

Figure 4
Binding isotherm for the interaction of *Nm*-Csp with single-stranded DNA along with the resulting Scatchard plot (insert). The nonlinear regression fit of the experimental data revealed a K_d of $1.25 \pm 0.04\ \mu M$ and revealed the stoichiometry of the protein–DNA complex to be 0.99 ± 0.01.

overall structure and ssDNA binding confirm that *Nm*-Csp belongs to the family of bacterial cold-shock proteins. Although the function of the protein remains to be determined, it seems unlikely that oligonucleotide binding occurs in the context of cold adaptation, since *N. meningitidis*, in contrast to *E. coli* and *Bacillus* spp., are not free-living bacteria but are commensal organisms that are resident in the human upper respiratory tract.

References

Bae, W., Xia, B., Inouye, M. & Severinov, K. (2000). *Proc. Natl Acad. Sci. USA*, **97**, 7784–7789.

Bennett, M. J., Schlunegger, M. P. & Eisenberg, D. (1995). *Protein Sci.* **4**, 2455–2468.

Berrow, N. S., Alderton, D., Sainsbury, S., Nettleship, J., Assenberg, R., Rahman, N., Stuart, D. I. & Owens, R. J. (2007). *Nucleic Acids Res.* **35**, e45.

Brünger, A. T., Adams, P. D., Clore, G. M., DeLano, W. L., Gros, P., Grosse-Kunstleve, R. W., Jiang, J.-S., Kuszewski, J., Nilges, M., Pannu, N. S., Read, R. J., Rice, L. M., Simonson, T. & Warren, G. L. (1998). *Acta Cryst.* D**54**, 905–921.

Geerlof, A. *et al.* (2006). *Acta Cryst.* D**62**, 1125–1136.

Jiang, W., Hou, Y. & Inouye, M. (1997). *J. Biol. Chem.* **272**, 196–202.

Jones, T. A., Zou, J.-Y., Cowan, S. W. & Kjeldgaard, M. (1991). *Acta Cryst.* A**47**, 110–119.

Kim, I., McKenna, S. A., Viani Puglisi, E. & Puglisi, J. D. (2007). *RNA*, **13**, 289–294.

Kremer, W., Schuler, B., Harrieder, S., Geyer, M., Gronwald, W., Welker, C., Jaenicke, R. & Kalbitzer, H. R. (2001). *Eur. J. Biochem.* **268**, 2527–2539.

Landsman, D. (1992). *Nucleic Acids Res.* **20**, 2861–2864.

Liu, Y. & Eisenberg, D. (2002). *Protein Sci.* **11**, 1285–1299.

Max, K. E., Zeeb, M., Bienert, R., Balbach, J. & Heinemann, U. (2006). *J. Mol. Biol.* **360**, 702–714.

Max, K. E., Zeeb, M., Bienert, R., Balbach, J. & Heinemann, U. (2007). *FEBS J.* **274**, 1265–1279.

Mueller, U., Perl, D., Schmid, F. X. & Heinemann, U. (2000). *J. Mol. Biol.* **297**, 975–988.

Newkirk, K., Feng, W., Jiang, W., Tejero, R., Emerson, S. D., Inouye, M. & Montelione, G. T. (1994). *Proc. Natl Acad. Sci. USA*, **91**, 5114–5118.

Schindelin, H., Jiang, W., Inouye, M. & Heinemann, U. (1994). *Proc. Natl Acad. Sci. USA*, **91**, 5119–5123.

Schnuchel, A., Wiltscheck, R., Czisch, M., Herrler, M., Willimsky, G., Graumann, P., Marahiel, M. A. & Holak, T. A. (1993). *Nature (London)*, **364**, 169–171.

Schroder, K., Graumann, P., Schnuchel, A., Holak, T. A. & Marahiel, M. A. (1995). *Mol. Microbiol.* **16**, 699–708.

Studier, F. W. (2005). *Protein Expr. Purif.* **41**, 207–234.

Terwilliger, T. C. (2000). *Acta Cryst.* D**56**, 965–972.

Terwilliger, T. C. & Berendzen, J. (1999). *Acta Cryst.* D**55**, 849–861.

Tettelin, H. *et al.* (2000). *Science*, **287**, 1809–1815.

Thieringer, H. A., Jones, P. G. & Inouye, M. (1998). *Bioessays*, **20**, 49–57.

Walter, T. S. *et al.* (2005). *Acta Cryst.* D**61**, 651–657.

Walter, T. S., Mancini, E. J., Kadlec, J., Graham, S. C., Assenberg, R., Ren, J., Sainsbury, S., Owens, R. J., Stuart, D. I., Grimes, J. M. & Harlos, K. (2008). *Acta Cryst.* F**64**, 14–18.

Zeeb, M. & Balbach, J. (2003). *Protein Sci.* **12**, 112–123.

Zeeb, M., Max, K. E., Weininger, U., Low, C., Sticht, H. & Balbach, J. (2006). *Nucleic Acids Res.* **34**, 4561–4571.